Dynamical Chaos of Plasma Ions in Electrostatic Waves

A. Fasoli, F. Skiff,[a] R. Kleiber, M. Q. Tran, and P. J. Paris

Centre de Recherches en Physique des Plasmas, Association EURATOM–Confédération Suisse, Ecole Polytechnique Fédérale de Lausanne, 21, Avenue des Bains, CH-1007 Lausanne, Switzerland

(Received 2 October 1992)

Chaos generated by the interaction between charged particles and electrostatic plasma waves has been observed in a linear magnetized plasma. The macroscopic wave properties, the kinetic ion dielectric response, and the microscopic heating mechanisms have been investigated via optical diagnostic techniques based on laser-induced fluorescence. Observations of test-particle dynamical evolution indicate an exponential separation of initially close ion trajectories.

PACS numbers: 52.50.Gj, 52.20.Dq, 52.35.Fp

Wave-induced dynamical chaos in plasmas is studied extensively because of its general interest as a paradigm of nonlinear dynamics and its possible direct applications in space and laboratory plasmas, such as anomalous transport, nonlinear heating, and particle acceleration [1].

Hamiltonian single-particle models are able to predict transitions to chaos in terms of wave amplitudes and spectra, based on the Chirikov overlap criterion and its recent refinements [2]. The validity of these results needs to be verified for the different scenarios, since all kinds of collective reponse, such as self-consistent effects (feedback action of chaotic particles on the waves) or nonlinear wave-wave interactions, necessarily neglected in the models, can play a crucial role.

It has been predicted theoretically and demonstrated experimentally that in a magnetized plasma a wave propagating obliquely with respect to the magnetic field can generate fast ion heating through chaos in particle orbits [3–5].

The case of two (or more) waves propagating at different phase velocities is predicted to be suitable for attaining global chaos [6,7]. In this case, the large number of resonances present in particle phase space lowers the threshold amplitude for the occurrence of chaos, increasing the efficiency of the stochastic heating mechanism. Relatively low amplitude fields, associated with linear plasma modes, could then cause very strong nonadiabatic particle responses.

In the experiment reported in this Letter we investigate the interaction between ions and electrostatic waves in a Q-machine plasma. In particular, our aim is to study the transition to chaos via integrated observations of the collective ion response (wave characteristics), of ion kinetic features (modification of distribution functions, time scale for heating), and of test particle orbits (phase-space transport).

The experiments are performed on the LMP (Linear Magnetized Plasma) barium Q machine [8] (Fig. 1), a uniformly magnetized plasma column characterized by ion and electron temperatures of the order of 0.2 eV and a low degree of spatial and temporal inhomogeneities (e.g., $\delta n/n < 1\%$, $\delta B_0/B_0 < 0.3\%$). Plasma density is in the 10^8–10^{10}-cm^{-3} range. The maximum axial B_0 field is 0.3 T ($f_{ci} \cong 30$ kHz). Sheath acceleration at the hot plate causes a supersonic ion drift $v_D \approx 10^5$ cm/s. Coulomb collision mean free paths are of the order of the machine length.

Electrostatic ion waves ($f \approx f_{ci}$) are launched by a capacitive antenna consisting of four rings surrounding the plasma column at variable relative distances and phases. The optimum coupling, corresponding to a matching between the antenna spectrum and the plasma dispersion relation, is obtained for an interring distance of 1 cm (the width of the rings is 1 cm) and relative phases $[\pi, -\pi, -\pi, \pi]$. The entire system is floating with respect to the plasma. To reduce direct electron losses in the near field region, the antenna rings have been covered by an insulating material.

The diagnostic system is based on the technique of laser-induced fluorescence [LIF] [9], which provides a direct measurement of the ion velocity distributions. The spatial and temporal resolutions (< 5 mm^3 and < 50 ns, respectively) allow local observations of the ion response at different points of the space-time wave pattern. In particular, by using phase-synchronous detection, ion density oscillations and perturbed distribution functions [derived from $f^1(v)$ or from selected components of $f^2(v)$] can be directly recorded. From a Vlasov model, the properties of the waves propagating in the plasma can then be deduced [10].

A single frequency is placed on the four-ring antenna in the laboratory frame. According to the direction of

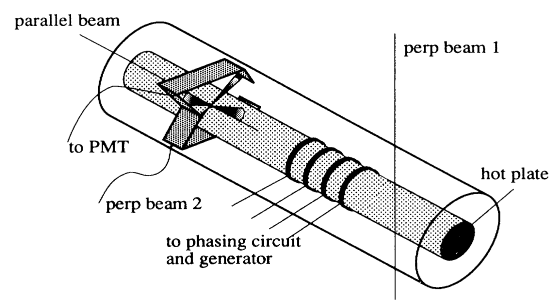

FIG. 1. The LMP experimental setup. The laser beams "perp 1" and "perp 2" are used to tag and detect test particles, respectively.

propagation in the plasma frame along the magnetic field, the wave frequency is Doppler shifted either up or down. Waves with two parallel phase velocities are observed, corresponding to the two propagation directions in the plasma frame. In addition, the upward Doppler shifted frequency has associated with it two perpendicular wavelengths corresponding to the two roots of the electrostatic ion cyclotron wave (EICW) dispersion relation [11,12]. At the frequency chosen for the experiment ($f=25$ kHz $\approx 1.15 f_{ci}$) the difference between the two parallel phase velocities is $\Delta v_\varphi = |v_{\varphi 2} - v_{\varphi 1}| \approx 5\times 10^4$ cm/s.

The Hamiltonian of a single magnetized particle in the field of these electrostatic modes can be written in the form

$$\begin{aligned} H = {} & p_z^2/2m + p_\phi \Omega + eV_1 \cos(k_{\parallel 1} z - \omega t + \eta_1) \\ & + eV_2 \cos(k_{\parallel 2} z - \omega t + k_{\perp 1} r + \eta_2) \\ & + eV_3 \cos(k_{\parallel 2} z - \omega t + \eta_3 + k_{\perp 2} r)\,. \end{aligned} \tag{1}$$

Here p_z and z stand for momentum and position along the magnetic field, r and ϕ for radial and angular cylindrical coordinates, and p_ϕ for the momentum conjugated to ϕ. Ω indicates the ion cyclotron angular frequency. V_1, V_2, V_3 are the potentials associated with the acoustic wave and the two components of the EIC wave. η_i ($i=1,2,3,$) are the initial phases. Clearly, for $V_i \neq 0$ ($i=1,2,3$), no transformation exists which would render H time independent: The energy is not a constant of the motion.

It is well known that for amplitudes $\{V_i\}$ exceeding a certain threshold value, a transition in the topology of particle orbits takes place: Ions are no longer trapped in the wave potential wells and wander chaotically in phase space.

In the case of one obliquely propagating wave the occurrence of chaos is linked to the nonlinear interaction of multiple Doppler shifted cyclotron resonances $\omega_n = \omega - k_\parallel v_D + n\Omega_{ci}$ ($n=0,\pm 1,\pm 2,\dots$). Here the situation is somewhat more complicated: In the parallel plane there are two primary resonances, at $v_{\phi 1}$ and $v_{\phi 2}$, and the series of harmonics associated with each one. For our experimental parameters, though, Δv_ϕ is such that on the parallel ion phase space one can consider only these primary resonances, neglecting, to a first approximation, the multiple island structure introduced by the nonzero perpendicular wave numbers. In expression (1), this implies $k_{\perp 1} = k_{\perp 2} = 0$ and $V_3 = 0$.

When the wave amplitude is such that the separatrices corresponding to the two primary resonances touch, a chaotic regime should be reached. As in Ref. [2] we introduce the stochasticity parameter $K = 2(A_1^{1/2} + A_2^{1/2})$, where $A_i = eV_i/m(\Delta v_\phi)^2$ is the normalized amplitude of the mode i ($i=1,2$). $K=1$ represents the threshold for the transition. For $K>1$ significant particle transport and acceleration should be triggered; macroscopically, fast ion heating should be achieved.

In Fig. 2 we plot the steady-state parallel and perpendicular ion temperatures as functions of the excitation amplitude. A threshold value exists, above which a significant heating occurs. A calibration of the wave amplitude based on the ion dielectric response [10] allows us to compare the observed threshold to the theoretical prediction for the experimental wave parameters. $K=1$ corresponds to the shaded area on the amplitude axis of the graph. We see that there is good agreement concerning the threshold for chaos, the main uncertainty being introduced by the measurement of the wave amplitudes. The same heating is observed in high-time-resolution measurements which are synchronized with the wave frequency so as to eliminate broadening of the observed distribution due to the reversible motion. No significant variations in the wave frequency spectrum are noticed when the excitation amplitude is increased above threshold.

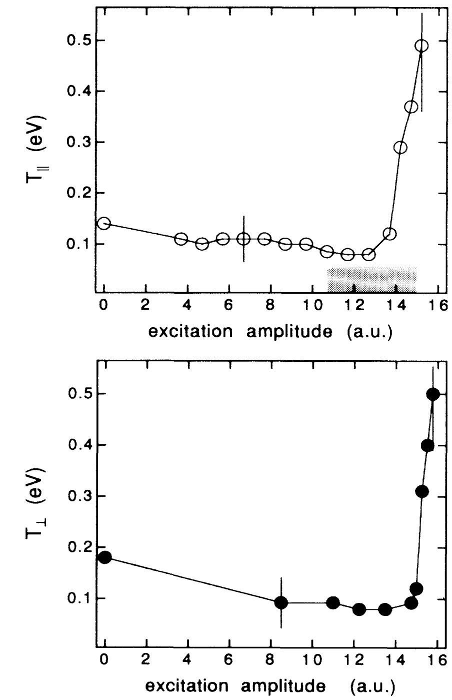

FIG. 2. Parallel (top) and perpendicular (bottom) ion temperatures vs wave excitation amplitude. $f=25$ kHz. These measurements, as well as those reported in the following graphs, have been taken a few cm downstream with respect to the antenna.

By gating the wave launching generator and observing the time-resolved ion distribution from the excitation start time, $t=0$, an accurate estimate of the heating time is possible. More specifically, by plotting the increase in the mean square velocity as a function of time, an estimate of the velocity-space diffusion coefficient averaged over all velocity classes can be obtained if the dependence is linear. This is shown in Fig. 3 for a wave amplitude just above threshold. The resulting velocity-space diffusion coefficient is more than 1 order of magnitude larger than the collisional coefficient [13]. The mechanism re-

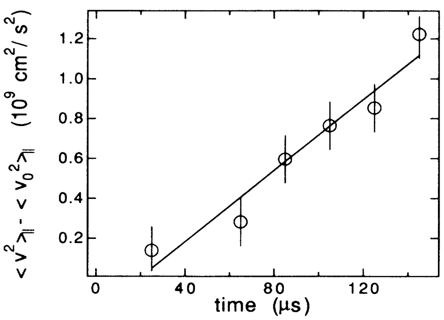

FIG. 3. Evaluation of the average parallel-velocity-space diffusion coefficient. $\langle v^2 \rangle_\parallel$ is the second-order moment of the parallel distribution function: $\langle v_0^2 \rangle_\parallel = \langle v^2 \rangle_\parallel (t=0)$. From the slope of the linear fit $D_{v_z v_z} \cong 1.1 \times 10^{13}\ cm^2/s^3$; the collisional diffusion coefficient for the same experimental parameters ($n \approx 10^9\ cm^{-3}$) would be [13] $D_{v_z v_z}^{coll} \approx 10^{12}\ cm^2/s^3$.

sponsible for the heating, therefore, is observationally distinct from collisional processes and is consistent with the operation of dynamical chaos.

A definite proof of this interpretation, and a rough estimate of the degree of chaos, can be achieved from an analysis of test-particle phase-space transport. An extension of LIF, optical tagging [14], has been used for this purpose. Spin polarization of ground-state ions, coupled with a particular scheme of LIF, allows the creation and detection of test particles [15]. The dynamical evolution of sets of tagged ions reveals information about the nature of ion orbits. In the case of a perpendicular tag beam injection geometry, the comparison of the tag signal radial profiles recorded at different locations in the plasma allows an estimate of ion transport mechanisms and parameters [16,17]. As shown in Ref. [17], the radial ion transport in the LMP unperturbed plasma is produced by purely classical mechanisms. By increasing progressively the wave amplitude from zero to values above the threshold for chaos, variations in diffusivity can be sought. No significant change is observed in the linear regime, but in the range corresponding to the threshold for heating an abrupt transition in the test-particle transport characteristics appears. The square of the width of the tagged particle profile no longer evolves linearly in time as in the case of diffusion (i.e., of a classical random walk), but it grows exponentially [Fig. 4(a)]. The z axis can be transformed into a time axis from the relation $t = z/v_D$. Likewise, the integral of the tag profile along the radial coordinate x_T, constant over the short distance spanned by the detection system in the low amplitude regime, decays exponentially [Fig. 4(b)]. It is important to observe that the two exponential rates are of the same order of magnitude ($\sim 1\ cm^{-1}$).

To operate a tag measurement corresponds to fixing an initial small volume in a subset of the particle phase space (in this case initial position and velocity in the perpendicular plane), and looking for it after a certain time. Here different final positions are explored, but only one

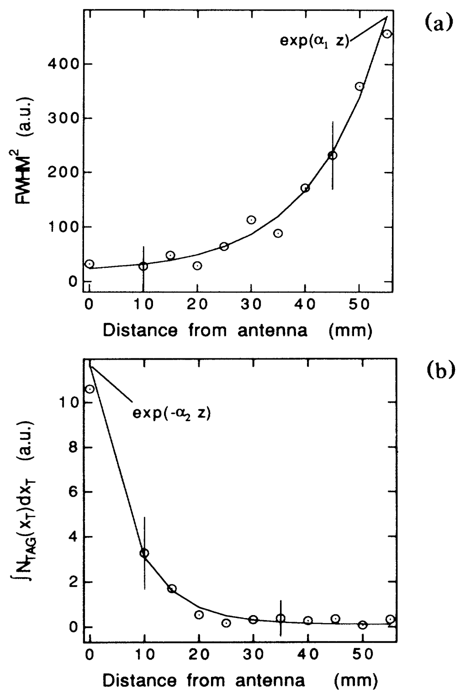

FIG. 4. (a) Square of the width of the tag signal radial profile, obtained by a radial scan of the tag injection point, vs the axial position. Note that, because of the uniform plasma parallel drift, the horizontal axis corresponds uniquely to the time axis in the plasma frame. (b) Total number of tagged particles (line integral of the tag signal radial profile) vs position. The best fit by an exponential curve, shown on the graphs, gives $\alpha_1 \cong 0.8\ cm^{-1}$, $\alpha_2 \cong 1.3\ cm^{-1}$.

perpendicular velocity is considered. Exponential broadening in space, in conjunction with the exponential decay of the line-integrated signal, is a signature of divergence of small volumes in phase space. Chaos, that is, local instability of orbits with respect to initial conditions, is therefore clearly indicated. The rate of divergence is also observed to increase as the wave amplitude is increased, as expected.

A qualitative comparison with an existing model can then be attempted. Small regions of phase space are predicted to evolve according to [18]

$$\Delta\Gamma \approx \Delta\Gamma_0 \exp(ht) , \tag{2}$$

where $\Delta\Gamma$ is the volume occupied (in a coarse-grain sense) at time t by particles which were in $\Delta\Gamma_0$ at time $t=0$. h is the so-called Kolmogorov-Sinai entropy, defined as the ensemble average of the sum of positive Lyapunov exponents:

$$h = \left\langle \sum_{\lambda_i > 0} \lambda_i \right\rangle \ (\lambda_i \text{ are Lyapunov exponents}) . \tag{3}$$

In the stochastic layer h is constant and is characterized by the same order of magnitude as the inverse of the correlation decay time τ_c: $h \approx \tau_c^{-1}$. In the case of the

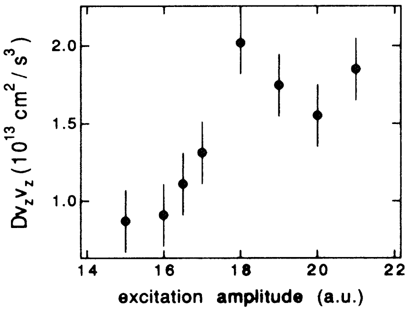

FIG. 5. Variations of the measured velocity-space diffusion coefficient with the excitation amplitude. A critical value for the amplitude, $V_c \cong 18$ a.u., at which saturation begins, can be defined.

two-wave-induced chaos an analytic estimate for τ_c is possible [18]:

$$\tau_c \approx [v_z \Delta k_\parallel \ln K]^{-1}. \tag{4}$$

For the parameters corresponding to the measurements reported in Fig. 4, expression (4) gives a correlation decay length of about 1 cm.

This value agrees with the observed divergence rate of test ion phase-space volume. Thus, even though more specific tagging measurements, allowing a reconstruction of the ion orbits [19], are necessary to evaluate directly the Lyapunov exponents, a first indication about the degree of stochasticity of the wave-driven chaotic system has been obtained.

At frequencies for which only one wave component along the magnetic field exists, no heating is observed, up to amplitudes where secular perturbations of the antenna and intrinsic nonlinearities become effective. In fact, the threshold for one obliquely propagating wave is expected to be higher than for waves with two parallel components. On the other hand, in the case of one purely parallel mode, the wave-particle dynamical system is integrable. The case of two waves is then experimentally shown to be more favorable in the achievement of chaos and stochastic heating.

By further increasing the amplitude of the waves well above threshold a different interaction regime can be explored and the question of the saturation of the particle energization mechanisms can be addressed. In Fig. 5 we see the dependence of the velocity-space diffusion coefficient upon the excitation amplitude, as deduced from the initial slope of the temperature versus time curve, in a gated measurement scheme. The data confirm the quadratice dependence for "moderate" amplitudes ($\leq V_c$) above threshold expected from quasilinear arguments [20], but at higher amplitudes a saturation takes place.

Preliminary results on wave propagation at amplitudes close to the threshold for chaos seem to indicate the presence of self-consistent effects, which tend to modify the wave spectrum. In fact, since ion orbits undergo a transition from regular to chaotic, the plasma wave fields, derived from the integration of charged-particle trajectories, are necessarily altered. These effects can be partially responsible for the observed saturation.

In summary, chaos in ion dynamics originated by the interaction between particles and electrostatic propagating plasma waves has been observed in a magnetized plasma. Optical measurements at different scales, from the single-particle to the macroscopic level, allowed a determination of the wave features, the kinetic ion response, and the plasma heating mechanism. Local transport analysis of test particles has indicated an exponential separation of initially close ion trajectories. A saturation of stochastic heating has been observed well above threshold; chaos appears to be self-limited.

This work was partially supported by the Fonds National pour la Recherche Scientifique.

[a]Permanent address: Laboratory for Plasma Research, University of Maryland, College Park, MD 20742.

[1] *Intrinsic Stochasticity in Plasmas,* edited by G. Laval and D. Grésillon (Editions de Physique, Orsay, 1979).
[2] D. F. Escande, Phys. Rep. **121**, 166 (1985).
[3] G. R. Smith and A. N. Kaufman, Phys. Rev. Lett. **34**, 1613 (1975).
[4] F. Skiff, F. Anderegg, and M. Q. Tran, Phys. Rev. Lett. **58**, 1430 (1987).
[5] J. M. McChesney, R. A. Stern, and P. M. Bellan, Phys. Rev. Lett. **59**, 1436 (1987).
[6] G. M. Zaslavsky *et al.*, Usp. Fiz. Nauk. **156**, 193 (1988) [Sov. Phys. Usp. **31**, 887 (1988)].
[7] P. Deeskow, K. Elsasser, and F. Jestczemski, Phys. Fluids **2**, 1551 (1987).
[8] P. J. Paris and N. Rynn, Rev. Sci. Instrum. **61**, 1096 (1990).
[9] R. A. Stern and J. A. Johnson III, Phys. Rev. Lett. **34**, 1548 (1975).
[10] F. Skiff and F. Anderegg, Phys. Rev. Lett. **59**, 896 (1987).
[11] J. P. M. Schmitt, Phys. Rev. Lett. **31**, 982 (1973).
[12] T. N. Good *et al.*, in *Proceedings of the Seventeenth EPS Conference on Controlled Fusion and Plasma Heating, Amsterdam, 1990, Europhysics Conference Abstracts*, edited by G. Briffod, A. Nijsen-Vis, and F. C. Schuller, (European Physical Society, Petit-Lancy, Switzerland), Vol. 14B, part IV, p. 1811.
[13] J. Bowles, R. McWilliams, and N. Rynn, Phys. Rev. Lett. **68**, 1144 (1992).
[14] R. A. Stern, D. N. Hill, and N. Rynn, Phys. Lett. **93A**, 127 (1983).
[15] F. Skiff *et al.*, Phys. Lett. A **137**, 57 (1989).
[16] R. McWilliams and M. Okubo, Phys. Fluids **30**, 2849 (1987).
[17] A. Fasoli *et al.*, Phys. Rev. Lett. **68**, 2925 (1992).
[18] R. Z. Sagdeev, D. A. Usikov, and G. M. Zaslavsky, *Nonlinear Physics* (Harwood Academic, Chur, 1988).
[19] A. Fasoli *et al.*, Phys. Rev. Lett. **63**, 2052 (1989).
[20] C. F. Carney, in *Intrinsic Stochasticity in Plasmas* (Ref. [1]), pp. 159–167.